Optical characterization of bulk $Zn_{1-x}Be_xTe$ crystals

2008 J. Phys.: Condens. Matter 20 255227

(http://iopscience.iop.org/0953-8984/20/25/255227)

IOP Publishing Journal of Physics: Condensed Matter

J. Phys.: Condens. Matter **20** (2008) 255227 (7pp) doi:10.1088/0953-8984/20/25/255227

Optical characterization of bulk $Zn_{1-x}Be_xTe$ crystals

Y C Shih[1], Y S Huang[1,4], F Firszt[2], S Łęgowski[2], H Męczyńska[2] and K K Tiong[3]

[1] Department of Electronic Engineering, National Taiwan University of Science and Technology, Taipei 106, Taiwan
[2] Institute of Physics, N Copernicus University, Grudziądzka 5/7, 87-100 Toruń, Poland
[3] Department of Electrical Engineering, National Taiwan Ocean University, Keelung 202, Taiwan

E-mail: ysh@mail.ntust.edu.tw

Received 21 February 2008, in final form 26 March 2008
Published 22 May 2008
Online at stacks.iop.org/JPhysCM/20/255227

Abstract

This paper presents an optical characterization of three bulk sphalerite $Zn_{1-x}Be_xTe$ crystals grown by the modified high pressure Bridgman method. The study was conducted in the near-band-edge interband transition regime using low temperature photoluminescence (PL), temperature-dependent contactless electroreflectance (CER) and/or photoreflectance (PR) in the temperature range of 15–400 K, and surface photovoltage spectroscopy (SPS) at room temperature. PL spectra at low temperatures of the samples investigated consist of an excitonic line, a band due to recombination of free electrons with holes located at shallow acceptors and a broad band related to recombination through deeper level defects. The band-edge excitonic transitions have been observed in the CER/PR spectra. The fundamental transition energies E_0 are determined via lineshape fits to the CER/PR spectra. The values of E_0 at room temperature obtained from CER/PR spectra correspond well to that determined from SPS measurements, and the Be contents x of the samples are determined using a linear equation which describes the room temperature band gap dependence on composition for the $Zn_{1-x}Be_xTe$ alloy system. The parameters describing the temperature dependence of the band-edge excitonic transition energies are evaluated and discussed.

1. Introduction

Theoretical studies [1, 2] have shown that beryllium could provide an attractive cationic substitution for ZnTe. A partial substitution of Zn by Be may improve the II–VI based device properties due to strong covalent bonding and high cohesive energy in beryllium chalcogenides [3–5]. Such a structure allows the extension of structural and band gap engineering of II–VI semiconductors towards lower lattice parameters and higher energy gaps. Beryllium has been used as a component of II–VI heterostructures for blue light-emitting diodes (LEDs), laser diodes (LDs) and photodetectors. There are a number of reports on the properties of bulk and layered (Zn, Be)Se solid solutions but relatively little information on tellurium based II–VI compounds with partial cationic substitution with Be atoms. Recent results have shown that $Zn_{1-x}Be_xTe$ is a promising material for a p-type cladding layer of ZnCdSe/MgZnCdSe LDs on InP substrate [6]. (Zn, Be)(Se, Te) has been successfully applied in the design of quantum wells [7]. ZnBeTe ternary alloy has been applied as a p-contact layer in II–VI LDs [8] and as a component of LEDs using an InP substrate [9]. High hole concentration (4.8×10^{18} cm^{-3}) has been achieved in $Zn_{0.6}Be_{0.4}Te$ layers exhibiting a band gap energy of 2.97 eV [6]. As for the design of optoelectronic devices based on heterostructures the knowledge of bulk crystal properties is of fundamental importance. Preliminary studies of photoluminescence (PL), basic crystallographic, thermal properties and photoacoustic (PA) spectra of bulk $Zn_{1-x}Be_xTe$ crystals have been reported [10–12].

This report deals with a detailed optical characterization of bulk sphalerite $Zn_{1-x}Be_xTe$ crystals using low temperature PL, contactless electroreflectance (CER) and photoreflectance (PR) in the temperature range of 15–400 K and room temperature

[4] Author to whom any correspondence should be addressed.

surface photovoltage spectroscopy (SPS). The bulk crystals of $Zn_{1-x}Be_xTe$ were grown by the modified high pressure Bridgman method from the melt. Low temperature PL spectra of the samples investigated consist of an excitonic feature, a band due to recombination of free electrons with holes located at shallow acceptors and a broad band with some structure related to recombination through deeper level defects. The band-edge excitonic transition energies E_0 are determined via lineshape fits to the CER/PR spectra. The Be contents of the samples are determined using a linear equation which describes the band gap dependence on composition for the $Zn_{1-x}Be_xTe$ alloy system. The parameters that describe the temperature dependence of the transition energy of the fundamental band-edge exciton are evaluated and discussed.

2. Experimental details

The $Zn_{1-x}Be_xTe$ crystals were grown from the melt by the high pressure Bridgman method [10]. The ZnTe and Te (purity 99.999%) and Be (purity 99.8%) powders were mixed and put into a graphite crucible. The intentional beryllium content ranged up to 0.15. The crucible containing the mixture was kept for three hours at a temperature of 1650 K, and then moved out of the heating zone at a rate of 2.4 mm h^{-1}. An argon overpressure of 11 MPa was maintained during the entire growth period. The crystal bar obtained was cut into plates of about 1 mm thickness and mechanically polished. The structure and composition of the sample were determined by x-ray methods [12]. X-ray investigations showed that the compound crystallizes in the sphalerite structure type. A linear dependence of the lattice constant on the alloy composition (Vegard's law) was assumed. The Be contents of the three $Zn_{1-x}Be_xTe$ samples, denoted as A, B and C, were determined as 0.6%, 6.5% and 12.1%, respectively.

To remove mechanical defects on the surface, the samples were mechanically polished using successively finer abrasives with the final polishing process using 0.05 μm aluminum oxide (Al_2O_3) powder. For optical measurements, the samples were additionally etched in a mixture of $K_2Cr_2O_7$:H_2SO_4:H_2O with a proportion of 3:2:1 followed by a treatment in CS_2 and 50% NaOH solution [13].

PL spectra were excited using the 325 nm line (~50 mW) of a He–Cd laser. The luminescence signals were analyzed by using a Jobin-Yvon 'TRIAX 550' spectrometer equipped with a 'SIMPHONY' charge coupled device (CCD) camera. The SPS measurements were done by using a metal–insulator–semiconductor (MIS) configuration with chopped light in air at room temperature. A static metal grid was used as a top electrode and the air gap between the metal grid and the sample was about 50 μm. The sample was mounted on a copper sample holder. A 150 W xenon arc lamp filtered by a 0.25 m monochromator provided the monochromatic light. The incident light intensity was maintained at a constant level of 10^{-5} W cm^{-2}. A beam splitter was placed in the path of the incident light. The intensity of this radiation was monitored by a power meter and was kept constant by a stepping motor connected to a variable neutral-density filter, which was also placed in the path of the incident beam.

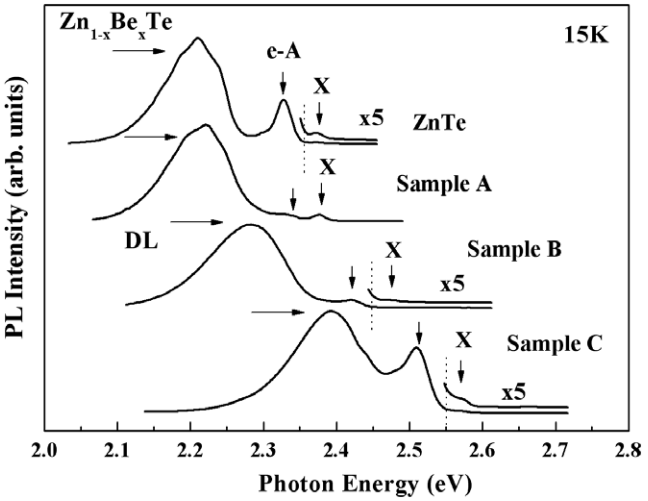

Figure 1. The PL spectra of ZnTe and three $Zn_{1-x}Be_xTe$ at 15 K. The band-edge excitonic line (X), free electron–shallow acceptor (e–A) emission and a band related to recombination through deeper level defects (DL) are indicated by arrows.

The chopping frequency was kept at 200 Hz. The induced surface photovoltage (SPV) on the metal grid was measured with a copper bottom as the ground electrode, using a buffer circuit and a lock-in amplifier. The CER/PR apparatus have been described in [14, 15]. In CER measurements, the ac modulating voltage was 1000 V peak to peak at 200 Hz. A mechanically chopped beam with frequency 200 Hz, 325 nm radiation (~1 mW) from a He–Cd laser was used as a pumping source for PR measurements. The temperature-dependent measurements were made between 15 and 400 K with the temperature stability of 0.5 K or better.

3. Results and discussion

Figure 1 presents the PL spectra of ZnTe and three $Zn_{1-x}Be_xTe$ samples with different Be contents at 15 K. The peak at 2.371 eV for ZnTe crystal is due to radiative recombination of excitons bound to neutral acceptors, which may be due to zinc vacancies [16] or Ag impurities [17]. The line at 2.325 eV is due to recombination of free electrons with holes located at shallow acceptors as a result of Li substituting for zinc in ZnTe lattices [18]. The weak peak at 2.3 eV is probably the LO phonon replica of the 2.325 eV line [18, 19]. The band with a prominent peak situated between 2.18 and 2.35 eV at ~2.2 eV is interpreted as due to deeper level donor–acceptor or free to bound recombination. The exact nature of the centers involved in this recombination process is unknown. According to literature data [16–20], the possible donors are Al substituting for Zn (Al_{Zn}) or tellurium vacancies (V_{Te}), and the acceptors are V_{Zn} or Ag_{Zn}. The emission band in the energy range from 2.0 to 2.3 eV was observed for intentionally undoped ZnTe bulk crystals [12, 21], as well as those doped with Al and Cl by thermal diffusion [17] and implanted with Al^+, Zn^+ and Ar^+ [16, 20]. The three main PL bands (2,371 eV, 2.325 eV and 2.2 eV in ZnTe) were observed for all $Zn_{1-x}Be_xTe$ crystals investigated. These emission bands

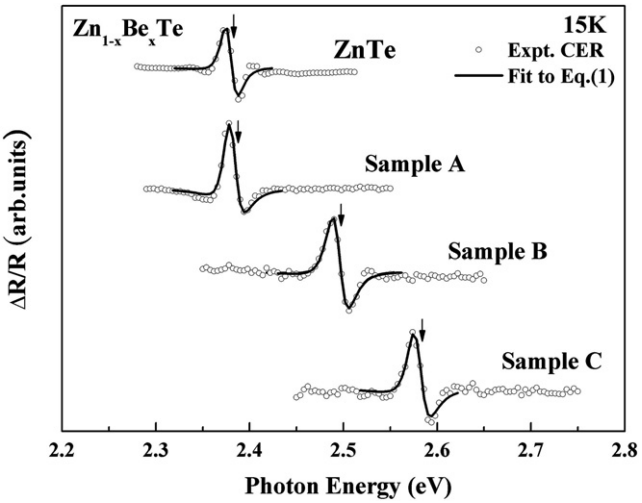

Figure 2. The CER spectra in the vicinity of band-edge regime of ZnTe and three $Zn_{1-x}Be_xSe$ samples at 15 K. The solid curves are least-squares fits to equation (1). The values obtained for the energies E_0 are indicated by the arrows.

positioned at 2.377, 2.33, 2.215 eV for sample A, 2.473, 2.42, 2.28 eV in sample B, and 2.566, 2.51, 2.39 eV for sample C are interpreted as due to radiative recombination of excitons bound to neutral acceptors (denoted as X), electrons from conduction bands with holes located at Li_{Zn} acceptors (e–A) and deeper level defect (DL) recombination, respectively.

Figure 2 illustrates the CER spectra in the vicinity of the band-edge regime of ZnTe and three $Zn_{1-x}Be_xSe$ samples at 15 K. The solid curves are least-squares fits to a derivative Lorentzian lineshape function of the form [22, 23]

$$\frac{\Delta R}{R} = \mathrm{Re}[Ae^{i\Phi}(E - E_0 + i\Gamma_0)^{-n}] \qquad (1)$$

where A and Φ are the amplitude and phase of the lineshape, E_0 and Γ_0 are the energy and broadening parameter of the band-edge excitonic transitions, and the value of n depends on the origin of the transitions. For the first-derivative functional form, $n = 2$ is appropriate for the bound states such as excitons and $n = 2.5$ is often used for bulk-like M_0 critical point transitions [22, 23]. We emphasize, however, that the position of the transition energy extracted from such a fit is relatively insensitive to the lineshape function. Our experimental signature E_0, indicated by the vertical arrow, is more consistent with the excitonic lineshape ($n = 2$). As shown in figure 2, at 15 K E_0 is located at 2.378 ± 0.003 eV for ZnTe. This feature exhibits blue-shifted character with increasing Be content and is positioned at 2.381 ± 0.003, 2.493 ± 0.003 and 2.579 ± 0.003 eV for samples A, B and C, respectively. The line broadening for the samples with higher Be content can be attributed in part to the alloy scattering effects and also to the poorer crystalline quality of the samples with higher content of Be.

A proper surface treatment of the sample must be performed to eliminate the damaged layer formed on the surface caused by mechanical polishing. The SPS technique can be utilized to check the condition of the surface layer [24].

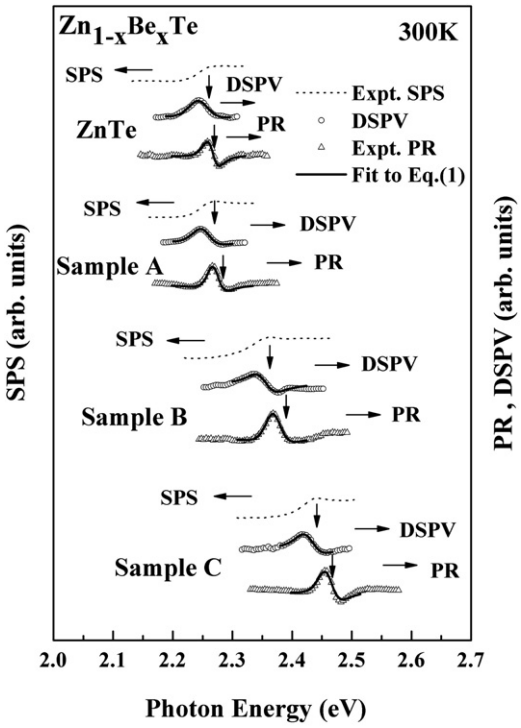

Figure 3. Room temperature experimental SPS and PR spectra as well as $(\Delta V_{SPS}/\Delta E)/V_{SPS}$ for ZnTe and three $Zn_{1-x}Be_xSe$ samples. The arrows show the energies E_0 obtained from DSPV and PR by least-squares fits to the first-derivative Lorentzian lineshape function (solid curves).

Figure 3 shows the surface photovoltage (SPV), and the first derivative of the SPV (DSPV) and PR spectra near the band edge at 300 K for ZnTe and three $Zn_{1-x}Be_xTe$ samples. Here the PR spectra (open triangle curves) are included for comparison purposes. The PR spectra are fitted to equation (1) (solid curves) and the band-edge transition energies are evaluated with an accuracy of a few meV. The values of E_0 obtained are indicated by arrows in the figure and listed in table 1. As shown in figure 3 the typical SPV spectrum (dashed curve) has a step-like shape, a typical characteristic for excitonic transitions, in the spectral region around the fundamental transition. In order to determine the values of the transition energies, we have numerically calculated the first derivative of the surface photovoltage signal with respect to photon energy ($\Delta V_{SPS}/\Delta E$) and then divided this quantity by the value of the photovoltage V_{SPS}. The ratio $(\Delta V_{SPS}/\Delta E)/V_{SPS}$ is proportional to $(\Delta\alpha/\Delta E)/\alpha$ [25], where α is the absorption coefficient. The derivative SPV (DSPV) curves obtained are displayed using open circles in figure 3. These data were fitted to the first derivative of a Lorentzian lineshape function, which is appropriate for excitonic transitions [26], and illustrated as solid curves in figure 3. The energies obtained are indicated by arrows and listed in table 1. It is noted that the values determined from SPS are smaller than that obtained from PR. Gal *et al* reported band gap determination for semiconductor samples via SPS [27]. Band gap values of 1.33, 1.41, and 1.68 eV were found for the InP, GaAs, and CdSe samples, respectively.

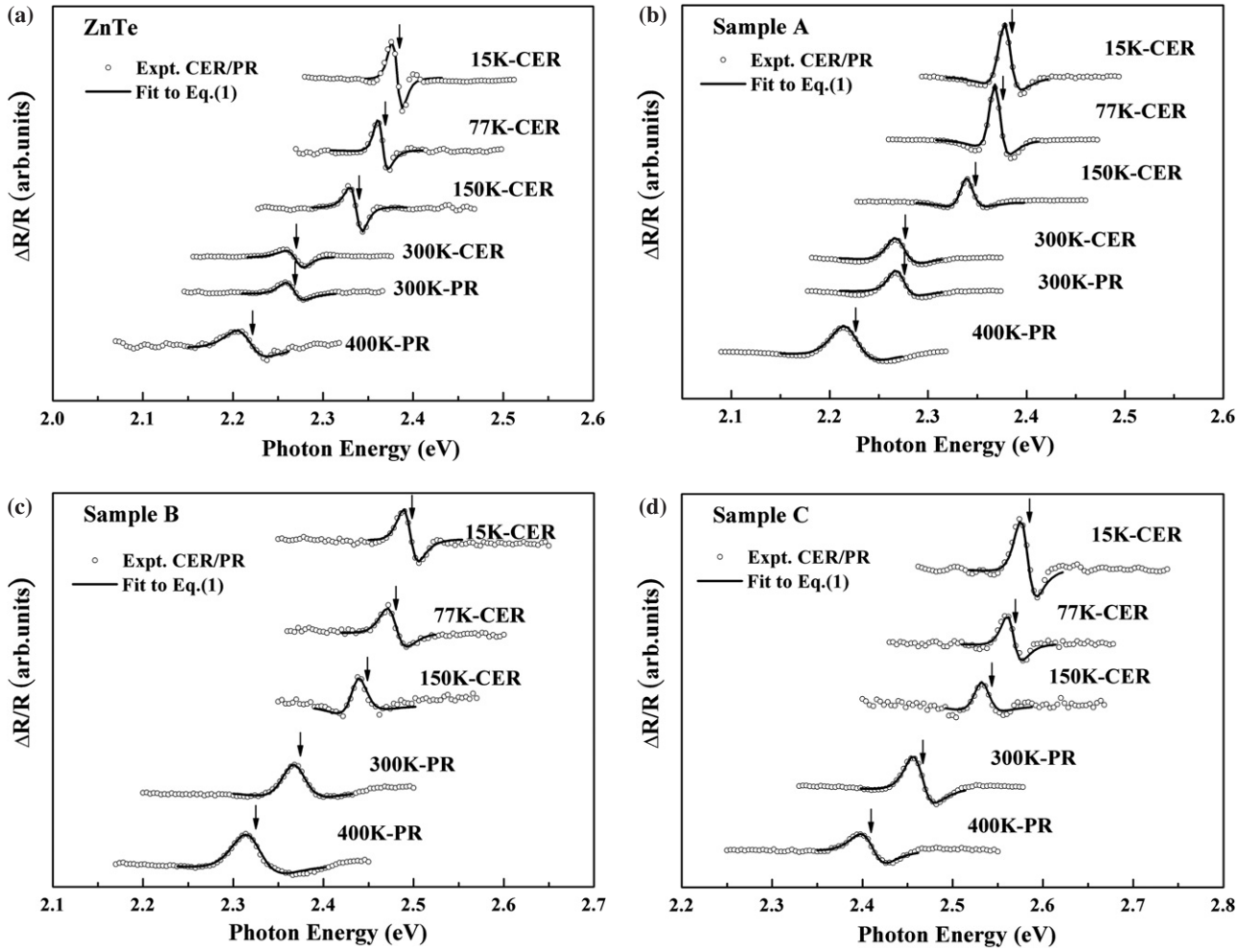

Figure 4. The experimental CER/PR spectra (open circle curves) of (a) ZnTe and $Zn_{1-x}Be_xSe$ samples (b) A, (c) B and (d) C at 15, 77, 150, 300 and 400 K. The solid curves are least-squares fits to equation (1). The values obtained for the energies E_0 are indicated by the arrows.

These values are slightly lower than the commonly accepted values of 1.34, 1.43, and 1.7 eV, respectively. The apparent reason for this discrepancy is the contribution of subband gap absorption in surface states. For comparison the energy gap values determined by the PA technique [11] from the same set of samples are also listed in table 1. It has been reported that the E_0 critical point is linearly dependent on the Be content x [28–30]. Taking the value of the direct band gap for BeTe from the literature (4.1 eV) [3] and the band gap of ZnTe obtained from PR (SPS) measurements, the contents of the Be are determined as 0.3% (0.3%), 5.6% (6.0%) and 10.6% (9.8%) for samples A, B and C respectively. These values are much smaller than that of the intentional beryllium fraction in the ingot and agree quite well with the values derived from the lattice constant via Vegard's law [12]. The discrepancies between the nominal composition of the ingot and that determined from Vegard's law may be caused by some excess of beryllium atoms located out of cationic positions because of the higher cation-to-anion ratio (measured by inductively coupled plasma mass spectrometry) for the crystals [12].

Displayed as the open circle curves in figures 4(a)–(d) are the experimental CER/PR spectra of ZnTe and $Zn_{1-x}Be_xTe$ samples A, B, and C, respectively, at 15, 77, 150, 300 and 400 K. As shown in figure 4, like for most semiconductors, when the temperature increases, the E_0 transition in CER/PR spectra exhibits a red-shift and lineshape broadening characteristics. The lineshape broadenings of the features are mainly due to the increase of electron (exciton)–phonon interaction effects. The full curves are least-squares fits to equation (1). The values of E_0 obtained are indicated by arrows in the figure.

Plotted using solid squares, circles and triangles in figure 5 are the temperature variations of E_0 obtained from CER/PR measurements with representative error bars for $Zn_{1-x}Be_xTe$ samples A, B and C, respectively. For comparison purposes, the band-edge excitonic peak positions X of low temperature PL spectra for $Zn_{1-x}Be_xTe$ samples A, B and C are also depicted in figure 5 using open squares, circles and triangles, respectively. The solid curves are least-squares fits to the Varshni semi-empirical relationship [31] as given by equation (2),

$$E_0(T) = E_0(0) - \frac{\alpha T^2}{(\beta + T)}. \qquad (2)$$

Table 1. Summary of the relevant parameters of ZnTe and three $Zn_{1-x}Be_xTe$ bulk crystal samples: intentional Be fraction in the ingot x_{ing}; Be composition derived from lattice constant $x_{x\text{-}ray}$ (Vegard's rule); energy gap value at room temperature and Be content determined from PR: $E_{0,PR}$, x_{PR}; SPS: $E_{0,SPS}$, x_{SPS}; photoacoustic (PA) technique: $E_{0,PA}$, x_{PA}.

Sample	x_{ing} (%)	$x_{x\text{-}ray}$ [a] (%)	$E_{0,PR}$ [b] (eV)	x_{PR} [b] (%)	$E_{0,SPS}$ [b] (eV)	x_{SPS} [b] (%)	$E_{0,PA}$ [c] (eV)	x_{PA} [c] (%)
ZnTe	0		2.264 ± 0.005		2.244 ± 0.005		2.28	
A	5	0.6	2.270 ± 0.005	0.3	2.249 ± 0.005	0.3	2.29	0.6
B	10	6.5	2.366 ± 0.005	5.6	2.355 ± 0.005	6.0	2.32	2.2
C	15	12.1	2.458 ± 0.005	10.6	2.426 ± 0.005	9.8	2.48	11.0

[a] Reference [12].
[b] Present work.
[c] Reference [11].

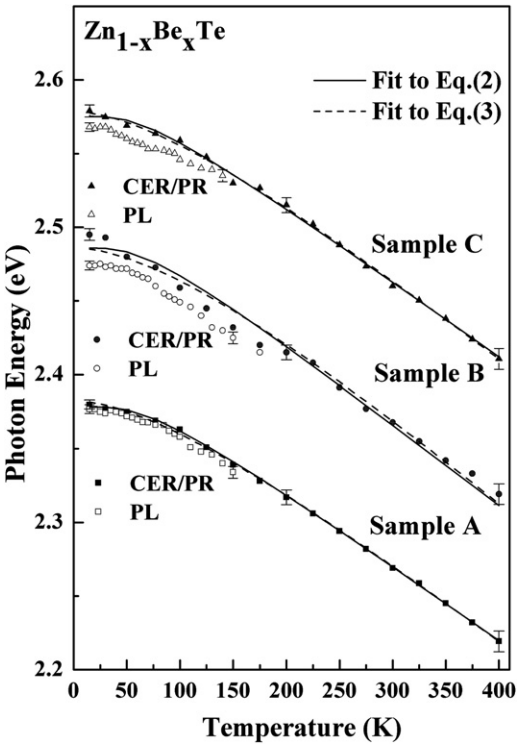

Figure 5. Temperature variation of the experimental values of E_0 with representative error bars for $Zn_{1-x}Be_xTe$ mixed crystal samples A, B and C. The solid curves are least-squares fits to equation (2) and the dashed curves are least-squares fits to equation (3).

Here E_0 (0) is the energy at 0 K; α and β are constants. The constant α is related to the electron (exciton)–average phonon interaction and β is closely related to the Debye temperature. The values obtained for $E_0(0)$, α and β are listed in table 2. For comparison, the parameters for bulk ZnTe and ZnTe films on GaAs [32, 33] are also listed in table 2.

The temperature dependence of the band-edge exciton transitions can also be described by a Bose–Einstein-type expression [34, 35]

$$E_0(T) = E_0(0) - 2a_B/[\exp(\Theta_B/T) - 1], \qquad (3)$$

where $E_0(0)$ is the transition energy at $T = 0$ K, a_B represents the strength of the electron (exciton)–average phonon interaction, and Θ_B corresponds to the average phonon temperature. Shown by the dashed curves in figure 5 are least-squares fits to equation (3). The values obtained for the various parameters are also given in table 2. For comparison purposes, the parameters for bulk ZnTe and ZnTe film on InP [36] are also listed in table 2. In addition the temperature dependences of the band gap variations dE_0/dT for $Zn_{1-x}Be_xTe$ films on InP [36] and ZnTe film on GaAs [37] are included in table 2.

As depicted in figure 5, it should be highlighted that for low Be content the transition energies E_0 obtained from CER/PR measurements correspond quite well to the peak positions of the band-edge excitonic features X in the PL spectra. A slightly different behavior is observed for $Zn_{1-x}Be_xTe$ crystals with high Be content. In the case of photoexcitation, excitons are generated over the entire absorption band range and then thermalized towards the bottom of the band in a time much shorter than the radiative lifetime of excitons. It is known that the absorption and reflectivity spectra reflect the energetic distribution of the density of excitonic states, while the luminescence spectra are determined by their degree of filling. The common feature of ternary II–VI solid solutions is, as observed at low temperatures, a shift of the exciton luminescence line towards lower energies as compared to that of the free exciton ground state determined from low temperature reflectivity spectra [38–40]. This feature is associated with exciton localization process due to compositional disorder. For the $Zn_{1-x}Be_xTe$ crystals with low Be content investigated (for example, sample A) the energetic position of the maximum of the excitonic PL line is shifted only a few meV towards lower energies from the corresponding energies E_0 determined from CER spectra in the temperature range from 15 to 150 K (see figure 5). The character of the temperature dependence of the energetic position of the PL excitonic peak follows the CER data. For higher Be content (sample B) however, the differences between exciton energies determined from CER and PL spectra become noticeably larger at low temperatures (at around 15 K) than at higher ones. This is different from the case for the data for sample A where the CER and PL data are almost the same. This indicates that some localization of excitons has taken place at low temperatures in $Zn_{1-x}Be_xTe$ crystals with large Be content.

The parameter α of equation (2) can be related to a_B and Θ_B in equation (3) by taking the high temperature limits of both expressions. This yields $\alpha = 2a_B/\Theta_B$. Comparison of the numbers presented in table 2 shows that this relation is indeed satisfied. From equation (3), it is straightforward to show that the high temperature limit of the slope of $E_0(T)$ versus T curve approaches the value of $-2a_B/\Theta_B$. The calculated

Table 2. Values of the Varshni-type and Bose–Einstein-type fitting parameters, which describe the temperature dependence of the band-edge transitions, and the temperature dependence of the band gap variation dE_0/dT for ZnTe and $Zn_{1-x}Be_xTe$.

Materials	$E_0(0)$ (eV)	α (10^{-4} eV K^{-1})	β (K)	a_B (meV)	Θ_B (K)	$-dE_0/dT$ (10^{-4} eV K^{-1})
ZnTe[a]	2.381 ± 0.001	5.6 ± 0.1	150 ± 10	28 ± 3	120 ± 10	4.7 ± 0.1
ZnTe[b]	2.3815	5.2	165			
ZnTe[c]	2.3745	5.4	150			
ZnTe[d]	2.381			11 ± 1	134 ± 11	3.2
ZnTe[e]	2.394 ± 0.4					4.53 ± 0.03
$Zn_{0.997}Be_{0.003}Te$[a]	2.382 ± 0.001	5.6 ± 0.1	150 ± 10	34 ± 3	140 ± 10	5.0 ± 0.1
$Zn_{0.944}Be_{0.056}Te$[a]	2.491 ± 0.001	5.9 ± 0.1	140 ± 10	36 ± 3	140 ± 10	4.9 ± 0.1
$Zn_{0.894}Be_{0.106}Te$[a]	2.578 ± 0.001	5.7 ± 0.1	140 ± 10	38 ± 3	150 ± 10	5.1 ± 0.1
$Zn_{0.94}Be_{0.06}Te$[e]	2.489					3.4
$Zn_{0.91}Be_{0.09}Te$[e]	2.547					3.4
$Zn_{0.86}Be_{0.14}Te$[e]	2.628					3.1
$Zn_{0.83}Be_{0.17}Te$[e]	2.680					3.4

[a] This work (bulk, contactless electroreflectance/photoreflectance).
[b] Reference [32] (film on GaAs, absorption).
[c] Reference [33] (film on GaAs, photoluminescence).
[d] Reference [37] (film on GaAs, absorption and reflectance).
[e] Reference [36] (films on InP, reflectance and photoluminescence).

values of $-2a_B/\Theta_B$ for ZnTe and samples A, B and C are equal to -0.47, -0.49, -0.51 and -0.51 meV K^{-1} respectively, which agree well with the values of $[dE_0(T)/dT] = -0.47$, -0.50, -0.49 and -0.51 meV K^{-1} as obtained from the linear extrapolation of the high temperature (200–400 K) CER/PR experimental data. As shown in table 2, the values of $dE_0(T)/dT$ for Be-incorporated samples are closer to that of ZnTe crystal and agreed with the value for ZnTe film on GaAs derived from temperature-dependent absorption measurements by Pässler *et al* [37]. Such a small variation is most probably due to the small amount of beryllium in the Be-incorporated samples. However, the values obtained here, which are for bulk samples, are much larger (∼50% larger) comparing with the $Zn_{1-x}Be_xTe$ thin films grown on InP substrates by Maksimov *et al* [36], where the decrease in temperature dependence of the band gap variation dE_0/dT is attributed to the lattice hardening effect of Be incorporation. More work needs to be done to verify whether the lattice hardening effect is responsible for such a decrease in the case of Be-incorporated thin films since no evidence can be found for bulk samples. We stipulate that the decreasing of the temperature variation of the band gap energy for Be-incorporated ZnTe thin films may partly be due to the inherent built-in strain between the films and the substrates.

4. Summary

In summary, the near band-edge transitions of three modified Bridgman-grown sphalerite structure-type $Zn_{1-x}Be_xTe$ mixed crystals have been carried out using low temperature PL, temperature-dependent CER and/or PR in the temperature range of 15–400 K, and SPS at room temperature. Room temperature SPS has been used primarily as a technique for checking the surface condition of the samples. PL spectra at low temperatures consist of a weak exciton feature, a band due to recombination of free electrons with holes located at shallow acceptors and a broad band related to recombination through deeper level defects. Comparison of PL and CER/PR data for $Zn_{1-x}Be_xTe$ samples shows that for a low Be content the peak positions of the excitonic emission features in the PL spectra correspond well to the transition energies E_0 determined for the CER measurements. For samples with higher Be contents, the PL results indicate that localization of excitons has taken place at low temperature. The Be contents x of the samples are determined using a linear equation which describes the room temperature band gap dependence on the composition for the $Zn_{1-x}Be_xTe$ alloy system. The temperature dependence of E_0 has been analyzed using Varshni-type and Bose–Einstein-type expressions. The parameters extracted from the two expressions by extending into the high temperature regime are found to agree reasonably well.

Acknowledgments

The authors acknowledge the support of the National Science Council of Taiwan under Project No NSC 96-2221-E-011-030 and NTUST-NCU International Joint Research Project No RP07-02. This work was also supported in part by the Committee for Scientific Research of Poland under grant No 1 P03B 092 27 (realized in 2004–2007).

References

[1] Dandrea R G and Duke C B 1994 *Appl. Phys. Lett.* **64** 2145
[2] Mensz P M 1994 *Appl. Phys. Lett.* **64** 2148
[3] Waag A, Fischer F, Lugauer H J, Litz Th, Laubender J, Lunz U, Zehnder U, Ossau W, Gerhardt T, Möller M and Landwehr G 1996 *J. Appl. Phys.* **80** 792
[4] Waag A, Fischer F, Lugauer H J, Litz Th, Gerhardt Th, Nürnberger J, Lunz U, Zehnder U, Ossau W, Landwehr G, Roos B and Richter H 1997 *Mater. Sci. Eng.* B **43** 65
[5] Maksimov O 2005 *Rev. Adv. Mater. Sci.* **9** 178
[6] Che S B, Nomura I, Shinozaki W, Kikuchi A, Shimomura K and Kishino K 2000 *J. Cryst. Growth* **214/215** 321

[7] Fischer F, Landwehr G, Litz Th, Lugauer H J, Zehnder U, Gerhardt Th, Ossau W and Waag A 1997 *J. Cryst. Growth* **175/176** 532
[8] Cho M W, Hong S K, Chang J H, Saeki S, Nakajima M and Yao T 2000 *J. Cryst. Growth* **214/215** 487
[9] Maksimov O, Guo S P and Tamargo M C 2002 *Phys. Status Solidi* b **229** 1005
[10] Firszt F, Łęgowski S, Męczyńska H, Szatkowski J, Banasiak A, Paszkowicz W, Falke U, Schultze S and Hietschold M 2000 *J. Cryst. Growth* **214/215** 880
[11] Firszt F, Łęgowski S, Męczyńska H, Szatkowski J and Zakrzewski J 2001 *Anal. Sci.* **17** S129
[12] Paszkowicz W, Firszt F, Łęgowski S, Męczyńska H, Zakrzewski J and Marczak M 2002 *Phys. Status Solidi* b **229** 57
[13] Firszt F, Wronkowska A A, Wronkowski A, Łęgowski S, Marasek A, Męczyńska H, Pawlak M, Paszkowicz W, Strzałkowski K and Zakrzewski A J 2005 *Cryst. Res. Technol.* **40** 386
[14] Hsu H P, Huang P J, Huang C T, Huang Y S, Firszt F, Łęgowski S, Męczyńska H, Strzałkowski K, Marasek A and Tiong K K 2008 *J. Appl. Phys.* **103** 013501
[15] Huang Y S and Pollak F H 2005 *Phys. Status Solidi* a **202** 1193
[16] Kwietniak M and Wardzyński W 1975 *Phys. Status Solidi* a **31** K47
[17] Tews H, Schneider M and Legros R 1983 *J. Appl. Phys.* **54** 677
[18] Crowder B L and Pettit G D 1969 *Phys. Rev.* **178** 1235
[19] Watanabe N and Usui S 1967 *Japan. J. Appl. Phys.* **6** 1253
[20] Bryant F J and Verity D 1981 *J. Lumin.* **22** 171
[21] Kwietniak M 1980 *Luminescence Phenomena in ZnTe* (Ossolineum, Wrocław: Polish Academy of Sciences)
[22] Aspnes D E and Studna A A 1973 *Phys. Rev.* B **7** 4605
[23] Pollak F H and Shen H 1993 *Mater. Sci. Eng.* R **10** 275
[24] Wang J Z, Huang P J, Hsu H P, Huang Y S, Firszt F, Łęgowski S, Męczyńska H, Marasek A and Tiong K K 2007 *J. Appl. Phys.* **101** 103539
[25] Kronik L and Shapira Y 2001 *Surf. Interface Anal.* **31** 954
[26] Aigouy L, Pollak F H, Petruzzello J and Shahzad K 1997 *Solid State Commun.* **102** 877
[27] Gal D, Mastai Y, Hodes G and Kronik L 1999 *J. Appl. Phys.* **86** 5573
[28] Maksimov O and Tamargo M C 2001 *Appl. Phys. Lett.* **79** 782
[29] Buckley M R, Peiris F C, Maksimov O, Muñoz M and Tamargo M C 2002 *Appl. Phys. Lett.* **81** 5156
[30] de Almeida J S and Ahuja R 2006 *Appl. Phys. Lett.* **89** 061913
[31] Varshni Y P 1967 *Physica (Utrecht)* **34** 149
[32] Langen B, Leiderer H, Limmer W, Gebhardt W, Ruff M and Rössler U 1990 *J. Cryst. Growth* **101** 718
[33] Yu Y M, Nam S, Lee K S, Choi Y D and O B 2001 *J. Appl. Phys.* **90** 807
[34] Logothetidis S, Cardona M, Lautenschlager P and Garriga M 1986 *Phys. Rev.* B **34** 2458
[35] Viña L, Logothetidis S and Cardona M 1984 *Phys. Rev.* B **30** 1979
[36] Maksimov O, Muñoz M, Samarth N and Tamargo M C 2004 *Thin Solid Films* **467** 88
[37] Pässler R, Griebl E, Riepl H, Lautner G, Bauer S, Preis H, Gebhardt W, Buda B, As D J, Schikora D, Lischka K, Papagelis K and Ves S 1999 *J. Appl. Phys.* **86** 4403
[38] Firszt F, Męczyńska H, Łęgowski S and Paszkowicz W 2004 *J. Alloys Compounds* **371** 107
[39] Mariette H, Triboulet R and Marfaing Y 1990 *J. Cryst. Growth* **86** 558
[40] Abdukadyrov A G, Baranovski S D, Verbin S Yu, Ivtchenko E L, Naumov A Yu and Resnizkii A N 1990 *Sov. Phys. JETP* **71** 1155